

# Cassini Camera Contamination Anomaly: Experiences and Lessons Learned

Vance R. Haemmerle<sup>1</sup> and James H. Gerhard<sup>2</sup>

*Jet Propulsion Laboratory, California Institute of Technology, Pasadena, California, 91109*

We discuss the contamination “Haze” anomaly for the Cassini Narrow Angle Camera (NAC), one of two optical telescopes that comprise the Imaging Science Subsystem (ISS). Cassini is a Saturn Orbiter with a 4-year nominal mission. The incident occurred in 2001, five months after Jupiter encounter during the Cruise phase and ironically at the resumption of planned maintenance decontamination cycles. The degraded optical performance was first identified by the Instrument Operations Team with the first ISS Saturn imaging six weeks later. A distinct haze of varying size from image to image marred the images of Saturn. A photometric star calibration of the Pleiades, 4 days after the incident, showed stars with halos. Analysis showed that while the halo’s intensity was only 1 - 2% of the intensity of the central peak of a star, the halo contained 30 - 70% of its integrated flux. This condition would impact science return. In a review of our experiences, we examine the contamination control plan, discuss the analysis of the limited data available and describe the one-year campaign to remove the haze from the camera. After several long conservative heating activities and interim analysis of their results, the contamination problem as measured by the camera’s point spread function was essentially back to pre-anomaly size and at a point where there would be more risk to continue. We stress the importance of the flexibility of operations and instrument design, the need to do early in-flight instrument calibration and continual monitoring of instrument performance.

## I. Introduction

NEARLY all scientific and navigation-related spacecraft instrumentation has to deal with the issue of contamination, especially those that have detector elements at cryogenic temperatures. Because instrument contamination can make the difference between a successful mission and one that fails or has degraded results, the spacecraft community has expended much effort to understand, characterize and prevent this hazard. Some missions, such as the Midcourse Space Experiment<sup>1</sup> and the Optical Properties Monitor on the Mir spacestation<sup>2</sup>, have flown with contamination monitoring equipment to better understand the issue. Spacecraft and instrument materials are chosen to minimize outgassing, vacuum bakeouts are done throughout the instrument building process and physical barriers are used to block contaminants from migrating. Still, despite these efforts at contamination control, instruments such as the Stardust Navigation Camera<sup>3</sup>, and Near Earth Asteroid Rendezvous (NEAR) continue to be plagued with events, which threaten their scientific return or operation.

Contamination of optical instruments can occur at all stages of a mission, from instrument fabrication, transportation, test, integration with the spacecraft, launch and in-flight. Sources of contamination on the ground can range from a fingerprint to contact with ground equipment. In-flight contamination can result from loose items during launch, ejection of covers, outgassing of instrument and spacecraft materials such as water, organics, silicones and propellant and the in-situ environment such as atomic oxygen in low Earth orbit or interplanetary dust or ring material. NASA’s Space Environments and Effects (SEE) Program has consolidated such information in its Satellite Contamination and Materials Outgassing Knowledgebase<sup>4</sup>.

The Jet Propulsion Laboratory’s Flight Project Practices document, section 6.10, has rules concerning the selection of materials and processes to be used in flight projects. Each project has to conduct an evaluation to identify the potential risks from particulate and molecular contamination to meeting scientific or mission requirements. If such a risk is found, the project is to develop and implement a contamination control program and a Contamination Control Plan.

---

<sup>1</sup> Senior Member of Technical Staff, Instrument Software Systems Section, Mail Stop 230-250.

<sup>2</sup> Member of Engineering Staff, Instrument Software Systems Section, Mail Stop 230-250.

## II. Cassini contamination control

The Cassini Cameras, called the Imaging Science Subsystem<sup>5</sup>, are one of 12 instrument packages aboard the Orbiter part of the Cassini-Huygens mission. ISS consists of two cameras, the Narrow Angle Camera (NAC), which is an  $f/10.5$  2000mm Ritchey-Chrétien reflective telescope with two filter wheels of 12 filters each covering the range of 200-1100 nanometers, and the Wide Angle Camera (WAC), which is an  $f/3.5$  200mm refractive telescope with 9 filters in each wheel covering the range of 380-1100 nanometers. Both cameras use a 1024x1024 element charged-coupled device (CCD) passively cooled by a radiator connected via a cold finger to 180K ( $-90^{\circ}\text{C}$ ) to minimize dark current.

Camera contamination mitigation from design conception through end-of-mission was the primary goal of the contamination control team assigned to the Cassini Imaging Science Subsystem. During the design of the cameras, effort was placed on selecting and using materials that were known to be a low contamination risk (either out-gassing or shedding) in the environment conditions that were faced during the mission. Suspect materials were tested in a vacuum chamber at various temperatures in the Molecular Contamination Investigation Facility (MCIF).

Special handling considerations were put into place during the assembly and testing phase of the cameras to minimize contaminants being introduced from external sources. Final assembly of the optics occurred in a clean room with a vertical down-flow tent. The optical assembly was under a nitrogen purge during non-assembly hours. Each camera subassembly was also baked out individually to both clean, and characterize the subassembly cleanliness. The cleanliness was determined by using a Thermoelectrically-Cooled Quartz Crystal Microbalance (TQCM) in each bake-out. The TQCM's measured the weight of thin films of solid materials down to a fraction of an Angstrom that would outgas from the subassemblies.

The contamination control plan for testing of the cameras after assembly was adopted from the Hubble Space Telescope WF/PC II. To maintain internal cleanliness of the ISS camera heads during transportation between tests and to the launch facility, a dry purge of nitrogen gas was used.

Requirements and allocations were established for ISS regarding allowable signal throughput degradation during mission lifetime due to molecular and particulate contamination from internal and external sources while in assembly, launch and flight environments. Estimates of these were calculated and compared to the established allocations. The estimated external molecular and particulate environments and the estimated internal particulate environment of ISS met the allocated requirements. However, the estimated internal molecular environment exceeded the allocated requirement, thus it necessitated in-flight procedures of decontamination. For

in-flight contamination mitigation, two sets of decontamination heaters were incorporated onto the cold finger/radiator assembly (Fig. 1). Before launch, two scenarios were being considered for in-flight contamination prevention. The first scenario required leaving the decontamination heaters on for the entire cruise. The second option required a periodic on-off cycling of the heaters throughout the cruise. The first scenario wasn't possible because of both power issues, as well as imaging requirements throughout the cruise part of the mission, which included Jupiter. The second option was accepted by both the project and the contamination control team and required turning decontamination heaters on for 14 hours, every six months. The periodic instrument maintenance (PIM) that was ultimately used was a 16-hour decontamination cycle every 90 days.

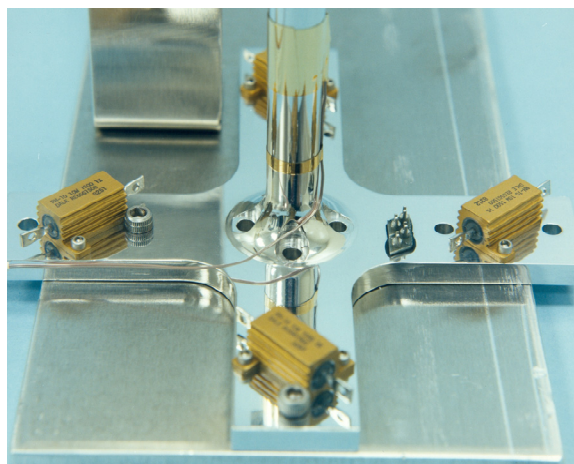


Figure 1. ISS heaters mounted on radiator struts.

## III. Decontamination

Under normal operation, the temperatures of the optical elements are kept within flight operating limits by appropriately placed active 'performance' heaters controlled by the flight software. The CCD package, overcooled by the radiator, is brought up to its operating temperature of  $\sim 183\text{K}$  ( $-90^{\circ}\text{C}$ ) and regulated by the CCD performance heater. The replacement heaters keep the optical elements and CCD within allowable non-operating temperature limits when the camera is off. The replacement heaters are controlled by the spacecraft and are not variable.

The CCD and radiator/cold finger are the coldest parts of the instrument. Thus, they are most susceptible to contamination. The decontamination heaters, which are attached to the radiator, are used to drive off volatile

contaminants off these components. For a full decontamination, both sets of heaters, Level 1 and 2 are on and the CCD reaches a temperature of  $\sim 303\text{K}$  ( $+30^\circ\text{C}$ ). During a full decontamination, the other parts of the instrument only increase a few degrees.

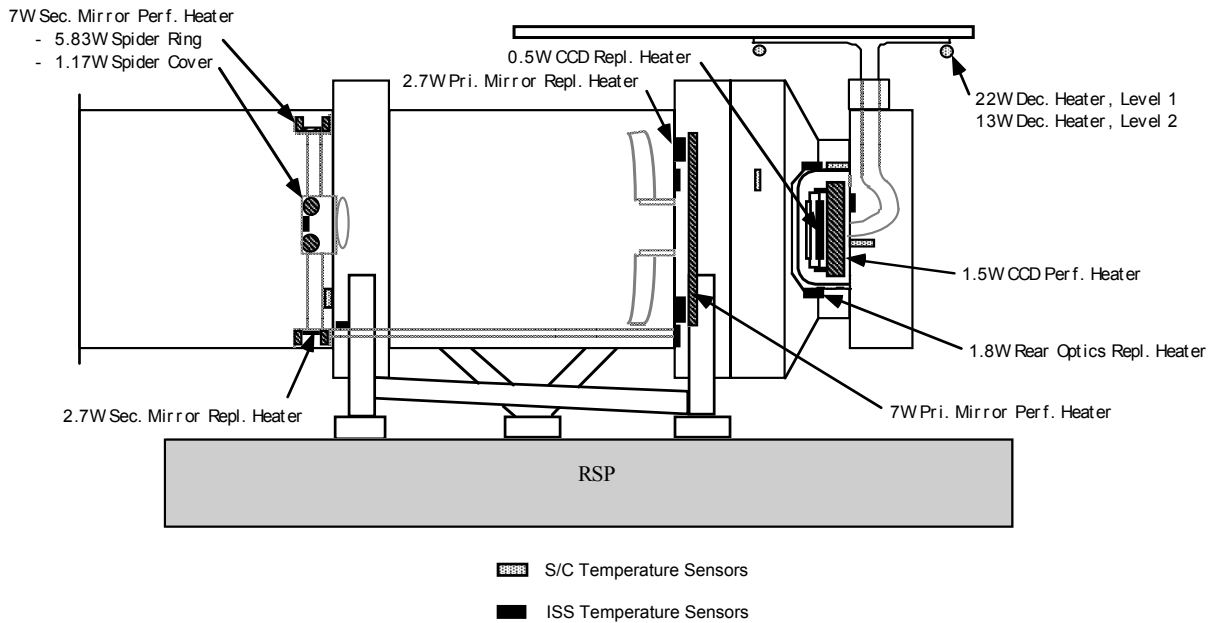


**Figure 2. Location of Decontamination, Performance and Replacement heaters on the NAC.**

From launch in 1997 until the Jupiter encounter in late 2000, except for a few observations, the instrument was off and the Level 1 decontamination and replacement heaters were on. This kept the CCD at  $\sim 273\text{K}$  ( $0^\circ\text{C}$ ) to anneal the CCD and protect it from radiation damage. When a PIM was done, the Level 2 heater was also turned on to reach  $+30^\circ\text{C}$ .

## IV. Haze anomaly

### A. Background

The extensive efforts to avoid contamination seemed to have paid off. The first Cassini Imaging test, Instrument Check Out (ICO-1) in January 1999, fourteen months after launch was nominal. Long exposures with the Moon off frame during Earth Swing-by in August 1999 showed that scattered light could be an issue under certain circumstances but the images of the Moon itself were sharp. From October 2000 to March 2001, Cassini conducted an exceptional encounter of Jupiter<sup>6</sup>. Over 25,000 images were taken and there was no sign of any contamination problem.

The Cassini Project employs a concept known as distributed operations<sup>7</sup>. Each instrument science team is responsible for the operation of their instrument from their home institution. However, Cassini ISS operations are a bit more complicated. ISS, along with three other instruments, is a Facility instrument in that it was built at JPL. There is a division of responsibilities between the science team and the ISS instrument operations (IO) team at JPL. The science team at its home institution, the Cassini Imaging Central Laboratory for Operations (CICLOPS), is responsible for designing observations and spacecraft pointing and passing their observation requests to the Cassini ISS operations team at JPL. The JPL team constraint checks and processes their requests into camera commands and loads. It also is responsible for instrument health and safety and anomaly resolution. Once the data is returned to the ground, the JPL team processes the raw telemetry packets into images, ancillary data and reports and sends them to CICLOPS. The science team has the responsibility to analyze and archive the data and publish their results.

Due to budgetary considerations, the development of the uplink and downlink ground data systems and sequence procedures was planned to occur during the Jupiter-Saturn cruise. The Jupiter encounter was not planned as part of the nominal mission and was done on a best effort basis. Much of the processing of these early observations had to be done manually and what tools did exist were immature and had limited functionality. This also applied to some of

the science team's tools such as their exposure estimation tool. Also, because of the division of responsibilities, the JPL team did not have access to the science team tools. Instrument calibration was also nominally planned to occur during the Jupiter-Saturn cruise. Because of the limited observation opportunities and the data volume allocations before and during the Jupiter encounter, the science team decided to maximize Jupiter observations and to postpone absolute in-flight calibration. After the Jupiter encounter, ISS scheduled a number of photometric observations of standard stars to calibrate the camera starting with C26 (cruise sequence 26, where each sequence is about 2 months long).

### B. Initial sighting

The first ever Cassini imaging of Saturn, the much anticipated ISS\_C27SA\_LRSATURN observation on Day of Year (DOY) 194, 2001 (Friday, July 13<sup>th</sup>) from 07:32 to 8:17 UT, obtained 51 NAC images of the Saturnian system in various filters and exposures. The data was downlinked the same day and products were created the following Monday, July 16<sup>th</sup>. Saturn's ring system is vertical in the images and five or six satellites are visible in some frames. However, a distinct haze around Saturn of varying size from image to image marks all of the images.

This haze was unexpected and was never seen before. After discussion within the ISS Instrument Operations (IO) team, the decision was made to write an Incident Surprise Anomaly (ISA) on the event. J. Gerhard submitted ISA Z71910 on July 23, 2001. C. Avis and V. Haemmerle investigated images from previous observations to determine whether they were similarly affected and when the problem began. Images of the star HD 339457 (SAO 88160) on DOY 145 did not show the haze, however images of the Pleiades on DOY 150 did. WAC images were also analyzed but did not show a problem. There were three support images for the Ultraviolet Imaging Spectrometer (UVIS) on DOY 148 that were taken with an exposure of 5ms, the lowest possible exposure. The star in the center of the images is very faint and the 8-bit TABLE encoding that was used results in a quantization of the background that makes any haze hard to see, but there appears to be evidence for a haze in these images also.

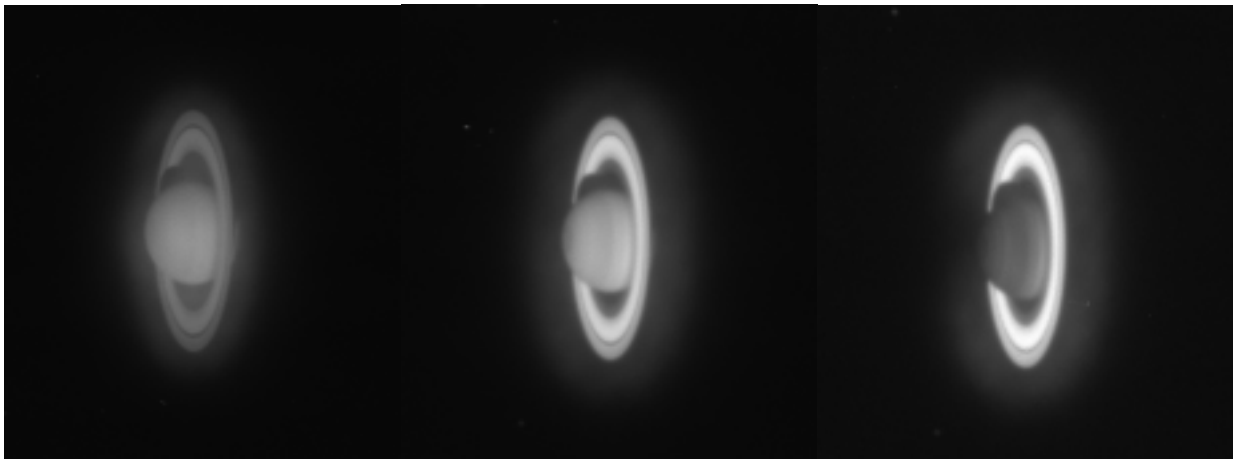


**Figure 3. Saturn images taken DOY 194, 2001. Filters from left to right: CL1/GRN, IR2/IR3 and CL1/MT3.**

Images of Vega on 2001/182 also display the haze.

Thus, the Saturn observations were 44 days after the first definite appearance of the haze. Several observations were done between DOY 150 and 194. Due to unfortunate timing, the ISS science team headquarters (CICLOPS) was executing a move to Boulder, CO from Tucson, AZ at the end of May 2001. This coincided with the May 31<sup>st</sup> delivery of the Pleiades images to the science team. Because science team members obtain their data from JPL through CICLOPS, they might not have had the data available to them during this unforeseen critical time. The team was also pre-occupied with the move.

Because no one was prepared to answer questions about the Haze problem, the opportunity to release the first Cassini images of Saturn was missed.

### C. Appearance

All of the Saturn images exhibited a haze surrounding the planet. This Saturn observation was the first extended object imaged since Jupiter and the only extended object in the several observations available showing the haze problem. Because the frames were taken in 8-bit TABLE mode, where the dynamic range of the 12-bit data is

compressed, it is easier to see both faint and bright features at the same time. This made the haze appear worse than it really was (when one converted back to actual 12-bit DN). Another thing that was noticed was that the amount of haze was different depending on which filter was used. Also the spatial extent of the haze was also different depending on filter. One can see this effect in Fig. 3 where the green (GRN) filter, on the left, shows less of a haze than the infrared and red images on the right.

#### D. Stellar images

The ISS photometric Pleiades observation was a very useful observation for determining the effect of the anomaly on the Point Spread Function (PSF). This observation contained images in both NAC and WAC cameras and used filters at a varied selection of wavelengths. The haze presents itself as a dim halo around the central peak of the star. The top two rows of Fig. 4 show stars before and after the appearance of the haze. The upper row compares Fomalhaut in CL1/GRN to Maia (SAO 76155), a Pleiades star, in the same filter. The second row compares HD 339457 in CL1/CL2 to Vega in CL1/CB3 in 12-bit mode. One can see that it is very hard to see the problem viewing raw 12bit DN. The bottom row shows the same Pleiades star in three different filter combinations revealing the relationship between the size of the halo and the wavelength of the light.

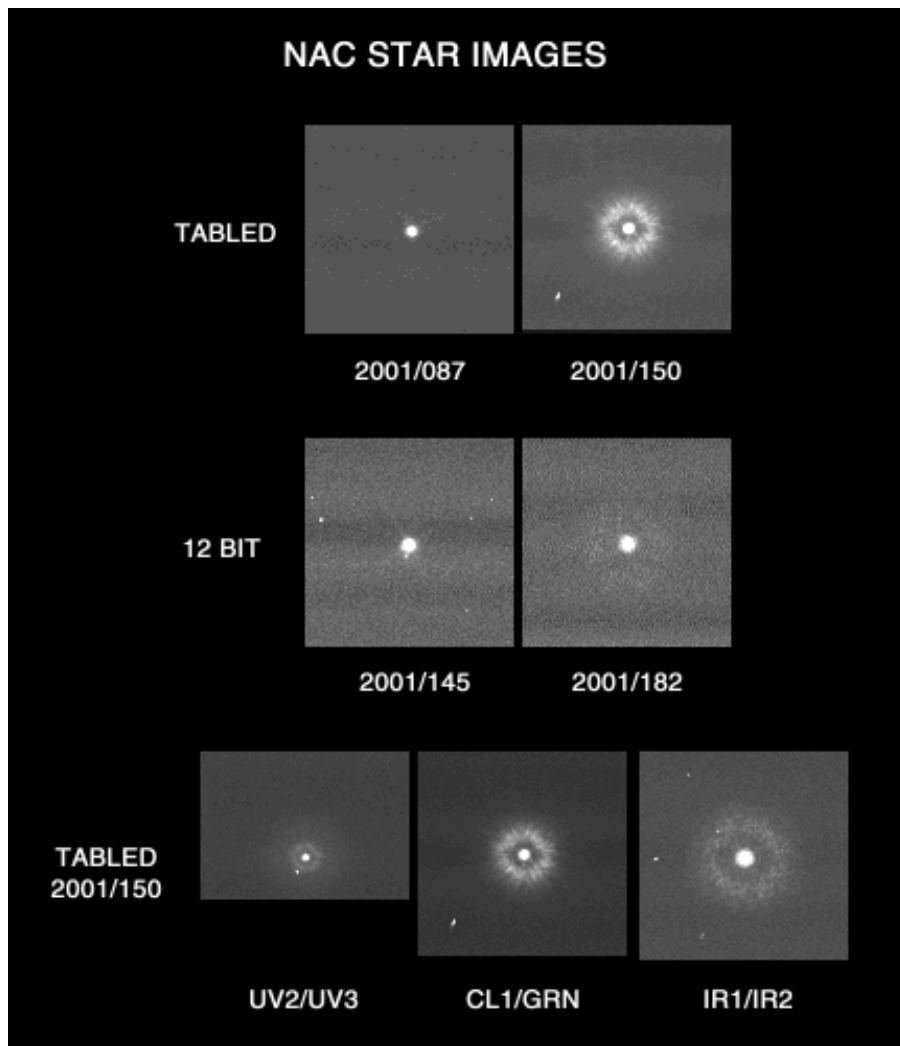


**Figure 4. Stellar images showing before and after the haze problem and the halo wavelength dependence.**

#### E. Timeline and data available

After the discovery of the problem, the first efforts were to locate as much imaging data as could be useful and to develop a timeline of all spacecraft and camera events during the time. The following ISS timeline was put together:

DOY	UT	Event
145	03:30	Photometric Calibration, ISS_C26ST_HD339001_PRIME (No haze)
145	18:00	Start 16 hour Periodic Instrument Maintenance (PIM)
146	10:00	End 16 hours Decontamination
147	07:30	Dark Frames, ISS_C26IC_DARK001_PRIME (No exposure)
148	10:15	UVIS support imaging, ISS_C26ST_EUVCHECK001 (Haze?)
150	10:50	Photometric Calibration, ISS_C26ST_PLEIADESN001_PRIME (Haze)

There were no suspect spacecraft events.

The data available were limited and had problems. Many of the DOY 150 Pleiades images showed only two stars, one, Maia was saturated in many, and the other was usually too dim. Missing lines marred most of the images. There was a Vega DOY 182 photometric calibration, but it was underexposed. There was also a DOY 192 Composite Infrared Spectrometer (CIRS) support imaging of the red supergiant star VY Canis Majoris as it drifted across the field of view; these were smeared slightly and the central peak of the star was saturated. There wasn't an opportunity to take more data to analyze the problem so the analysis had to use the existing data.

## F. Results of analysis

Due to the circular nature of the extended halo, a modified aperture photometry analysis lent itself as a good way to analyze the degree of point spread function degradation and characterization of the problem. A literature search was done and people from the Stardust and NEAR were contacted to learn about their problems and their possible similarity to ours. A team was put together containing people from Instrument Operations, the ISS operations lead, the camera system engineer and two people who had been on the contamination, one of whom was retired.

A meeting was held on August 15<sup>th</sup>, 2001 and the team reached a number of conclusions. Thankfully, the NAC problem was much less severe than either the Stardust or NEAR incidents. Focus problems, spacecraft propellant and the Jupiter Environment were all ruled out. It was also determined that the problem was not getting worse with time.

Concerning the stellar images, the central peak of a star appeared normal and the intensity of the halo was only 1-2% the brightness of the central peak. However because of spatial extent of the halo, it actually contained a large fraction of the stellar flux - from 30% in the infrared to 70% in the blue and ultraviolet. The size of the halo ranged from 5 pixels in radius in the ultraviolet to up to 20 pixels in the infrared (see Fig. 4). Thus, this would have a large impact on the scientific return of the NAC. The properties of the point-spread function were consistent with the contamination by very small particles on a transmissive surface causing a diffraction pattern in images of point source objects. The surface involved could have been the filter assembly or the CCD window. An interesting side note was that Ellis Miner, the Cassini Science Advisor, related that his early graduate work involved measuring diffraction patterns in an entirely different field, medicine<sup>8</sup>.

All evidence pointed to the PIM as the cause of the problem. There were many PIMs before this one without incident. In fact, this was the 13<sup>th</sup> ISS PIM of the mission. It was determined that there was nothing noteworthy about the temperature profiles of this decontamination in the sense that nothing went wrong. But there were two things that made this one unique. This was the first decontamination done since before the Jupiter Encounter in C19 on 2000/113 (April 22), i.e. the first decontamination in 13 months, which was more time for contaminants to have buildup. It also turned out to have been the first in-flight decontamination that started from -90°C instead of from around 0°C. This PIM had a temperature swing of 120°C in a short period of time instead of just 30°C. Large temperature swings are known to be related to contamination causes. Ref. 4, section 4.4.2.1 says

Terminator crossings, especially the portion when the spacecraft goes from dark to solar illumination, has been observed to generate the most water vapor and has been positively correlated with particle generation, possibly due to a mechanical 'deflection' effect due to thermal shock.

A review found two interesting and possibly relevant items. The first was that the radiators of the cameras had been resized with thermal blankets during integration with the spacecraft and had not been subsequently baked out. The thermal blankets used had been baked out, but of course the tape that was used was not. Secondly, a memo was found from 1995 from the contamination engineer to the thermal blanket engineer recommending that the CCD vent tube be extended. Due to a personnel change this action was not taken. This was a suspected contamination path.

Because the problem was not getting worse and the start of Approach Science was still two years away, Project management decided there was plenty of time for a solution and no immediate action was necessary. The earliest ISS imaging that was available to change was 60 days away, in sequence C28, and was another UVIS support activity. Since changing the pointing of the spacecraft requires much lead-time and extra work and not to impose on the UVIS observation, it was decided to use the target of the UVIS observation.

## V. Remediation

The solution to a problem can be puzzling when the most straightforward fix turns out to be the cause of the problem. Another full decontamination could make the problem worse before it got better – if it got better. It was



Figure 5. Color image of Maia.

decided that a week-long conservative decontamination cycle be conducted with only the Level 1 set of decontamination heaters on during its duration. That is, to have the CCD at a temperature which had proved to be safe for a majority of the cruise.

Before this activity occurred, a photometric observation of the stars 77 and 78 Tau on DOY 244 (September 1<sup>st</sup>) showed that the problem was still there and had not changed.

#### A. C28 Activity

The UVIS support activity in C28 involved having the spacecraft trace out a 3x3 mosaic centered on the star Spica (Alpha Vir). A NAC and WAC image was to be taken at each position an additional pair was also to be taken. The purpose of the support imaging was to determine the relative pointing between ISS and UVIS and to determine the UVIS field of view. Because of the size of the mosaic, only the central position would have Spica in the NAC frame which has 1/10 the field of view of the WAC. The planned observation had each image in the clear (CL1/CL2) filter. The amount of data allocated for use (datavolume) for this observation was limited to the number of images initially planned, so none could be added.

ISS Instrument Operations got approval from UVIS to change this observation. All 9 NACs in the mosaic instead would be taken at the central position. Also, as luck would have it, Spica was one of three stars imaged before the anomaly. It was the target during Instrument Checkout (ICO-1) in 1999. This provided the opportunity to image the same star in the same filters before and after the haze problem. Ten filter combinations were chosen from the ICO-1 observation to reasonably expose the star and span the maximum wavelength range. IO did not have the software to generate the observation request that our uplink processing used so a spreadsheet of the requested filters was sent to the ISS science team, which generated the request. As earlier discussed, a weeklong decontamination with the Level 1 heaters was done.

The decontamination cycle began on DOY 291 (October 18, 2001) and ended on DOY 298 (October 25). The temperature that the CCD reached was 266K ( $-7^{\circ}\text{C}$ ), which is lower than the cruise temperature because the replacement heaters were not on but the camera electronics were. The decontamination was completed a day before the imaging was done on DOY 299.

The results revealed that overall a change for the better had occurred over all wavelengths measured. The image in Fig. 6 shows a stellar image in the BL1/CL2 filter after the C28 decontamination. The image is contrast enhanced to show the faint extended light.

Our obvious conclusion was that for this filter, the character of the anomaly had changed -- the halo was gone or has collapsed into the central peak of the star. All filters except Ultraviolet no longer had a halo. Measurements showed that for this filter combination, where approximately 68% of the light was outside a radius of 5 pixels, now it was only 44%. The ~40% figure was about the same in the Ultraviolet, Blue, Green, Red as well as the Infrared. The lack of the formally strong wavelength dependence was perhaps due to the evaporation of the small particles or coalescing of them into larger particles. A measure of the width of the DN distribution gives 1.36 pixels for pre-anomaly, 10.03 pixels after the anomaly and 7.94 pixels after the C28 decontamination. This width improved by factors of 20-50% over the other filters. The comparison between these images and the ICO-1 images showed that the amount of light lost to scattering and absorption was at most a few percent.



Figure 6. After C28.

The fact that a change occurred at  $-7^{\circ}\text{C}$  confirmed to us that the contamination was indeed close to the CCD area (which was the only area to undergo a significant change in temperature), perhaps in the CCD package itself. The temperature of the primary and secondary mirrors underwent little change in this decontamination cycle. The fact that a change occurred at  $-7^{\circ}\text{C}$  gave us hope that the situation could be further improved by additional decontaminations or slightly higher temperatures, e.g. by turning on replacement heaters in the next decontamination test.

A meeting was held on November 16<sup>th</sup> to discuss the results. It was decided to repeat the experiment at a slightly higher temperature. The only three choices to increase the temperature short of having both decontamination heaters on were to a) turn on the Replacement heaters, b) use the CCD performance heater fully rather than have it regulate the temperature or c) do both. The contamination experts wanted to reach the temperature at which the Stardust contamination was removed but that was not possible with the possible heater combinations. Water was ruled out as a contaminant since it should have evaporated. There was some concern that the contamination might be evaporating at the higher temperature and then re-condensing when the CCD cooled to  $-90^{\circ}\text{C}$  again. It was decided to take images at a halfway point to check.

**B. C30 Activity**

The first decontamination that was able to be fully planned took place in January 2002, in cruise sequence C30, and was similar to the C28 decontamination but with all the images taken in full 12-bit mode and with ~ -40°C stopover images (using smaller Level 2 heaters alone) as well as the addition of the NAC's replacement heaters being on. Spica was chosen to be the target for all future decontaminations to have a constant reference.

The decontamination cycle began on DOY 022 (January 22) and ended on DOY 030 (January 30). Four sets of images were taken, two before and two after the weeklong activity. The temperature that the CCD reached was 277K (+4°C).

The replacement heaters were used to further raise the CCD temperature since -7°C wasn't warm enough to completely remove the contaminants. The replacement heater set includes a 0.5W CCD heater that provided the extra heat. The CCD performance heater did not operate since the CCD was already above its target of -90°C.

In C28, the camera heating was due to the heating of the cold finger attached to the CCD package, which just affected the CCD and surrounding area. Because the Replacement heaters are an all or none proposition, the use of them caused other parts of the camera to heat as well, by about 20°C.

The images from C30 revealed that the optical performance of the NAC continued to improve over all wavelengths measured. The images in Fig. 7 show stellar images before and after the C30 decontamination (and after the C33, see below). The images in each filter are all contrast enhanced in the same manner to show the faint extended light. However, because of the different brightness of Spica in the various filters, one should not compare filter-to-filter, but only before and after in the same filter.

Measurements showed that for the BL1/CL2 combination, where approximately 68% of the light was outside a radius of 5 pixels initially, then, after C28, 44% of the light was, the figure decreased to 18%. The ~20% value was about the same in the Ultraviolet, Blue, Green, Red as well as the Infrared.

It is interesting to note that originally images in the Infrared were least affected by the contamination measured in this way. In the course of activities to remove contamination, the shorter wavelength filters improved enough to surpass the Infrared, which then had the highest percentage. This is likely indicative of the removal of the smaller particles of contamination.

**Table 1. CCD Temperature with Level 1 heaters ON.**

Camera	Replacement Heaters	CCD temperature
OFF	OFF*	*Replacements must be ON
ON	OFF	-7°C
OFF	ON	+0°C
ON	ON	+4°C

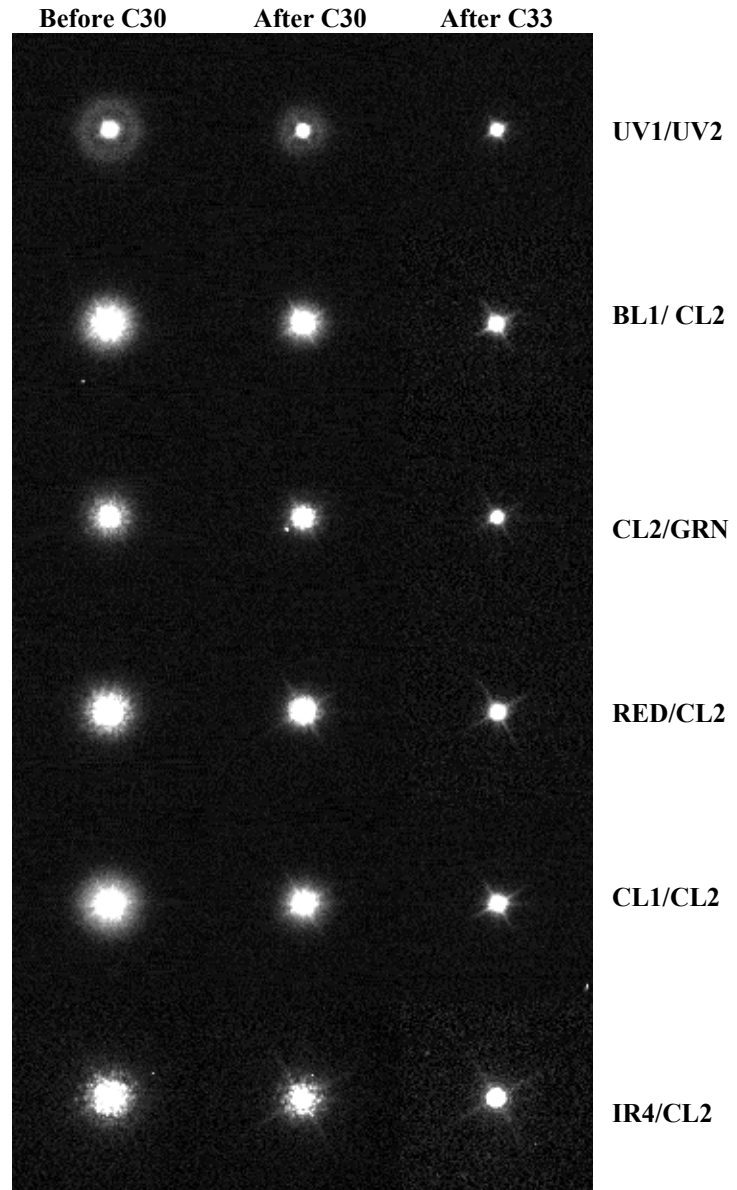


**Figure 7. Size improvement in various filters.**

Also interesting is that even the  $-90^{\circ}\text{C}$  C30 baseline images showed some small improvement compared to the 3-month earlier C28 images. The camera's CCD stayed at  $-90^{\circ}\text{C}$  during this interval. No improvement was seen between the start of the anomaly and the observation of 77 and 78 Tau about 100 days later, the last observation before the C28 decontamination.

The size of the stellar profiles was also clearly improving. A measure of the width of the DN distribution for BL1/CL2 gave 4.78 pixels. Measured in this way, the width of a star in many of the filter combinations was under half the size of the original anomaly. One can notice that the Ultraviolet filter still showed a slight halo.

Because ISS IO does not do spacecraft pointing, the request to point to Spica was sent to the ISS Science Team. Due to errors in the pointing files submitted by the Science Team, images of Spica were almost off the frame. ISA Z73572 was written on this issue. It turned out that the Right Ascension and Declination values used were truncated. We had expected that the same pointing as was done in ICO-1 or the UVIS support imaging would be used. Luckily, Spica was far enough from the edge of the frame so that the analysis could still be done.

Because of the improvement in the images, the peak brightness of the star increased from between 25% to 60%. This caused Spica to saturate slightly in two of the filter combinations and required an adjustment in exposure times for the next activity.

The C30 decontamination activity was the first time in flight that images were taken at a CCD temperature near  $-40^{\circ}\text{C}$ . At this warmer temperature, thermally generated dark current and "hot" pixels (which cause the vertical streaks upon CCD readout) are more active. Taking images near  $-40^{\circ}\text{C}$  allowed us to examine if the camera was re-contaminating upon cool-down. The analysis showed it was not. Stellar image properties at  $-40^{\circ}\text{C}$  are very similar to those at  $-90^{\circ}\text{C}$  though slightly poorer ( $\sim 0.2$  pixels larger). Despite higher dark current and hot pixels, they were still useful for analysis and comparison with  $-90^{\circ}\text{C}$  images. Each time we did a decontamination cycle from  $-90^{\circ}\text{C}$  to  $0^{\circ}\text{C}$  we took a thermal cycle. Thermal cycles were defined as a change of more than  $50^{\circ}\text{C}$  and they are treated as a consumable with a certain number allocated for the whole tour. The fact that we could stay at  $-40^{\circ}\text{C}$  between activities meant that we could minimize thermal cycles in future activities.

A meeting was held on February 12<sup>th</sup> to discuss the results. There was a 21-day decontamination planned for C32 whose results would determine the heater use in a C33 activity. However, because of the lag in analysis feeding back into sequence planning, the large lead time involved in any changes, and the failure of the two decontamination activities to fully remove the haze, members of the Science Team began to worry that perhaps the problem would not be cleared up before the Space Science phase where more extensive instrument calibration would be done. This phase was to begin in mid-2003.

In order to be more aggressive, Cassini IO/ISS proposed turning on heaters for the later part of C30 and throughout most of C31 in a very long replay of the successful C30 activity. This would involve turning on heaters to raise the CCD temperature to  $\sim +4^{\circ}\text{C}$  at the next reasonable uplink and keep them on until near the end of C31. This was possible because the activity would not require any datavolume or pointing. The C32 baseline images would show the result of a  $\sim 60$  to 80-day decontamination before the start of the already planned 21-day activity. Trajectory Correction Maneuver (TCM) 18 was scheduled to occur on April 3<sup>rd</sup> during C31. There was a concern that this option many not be allowed. Previously there was a requirement that decontamination heaters were to be off during TCMs, but this requirement was waived once the Spacecraft was past 3.9AU from the Sun.

An analysis was done of how much datavolume and time our activities were actually using compared to what was allocated. Because there was room for more images and it was decided to add some long exposures to bring up the very low-level structure in the point spread function that could be compared to ISS Fomalhaut saturation observations from September 2000. It turned out there was a Visual and Infrared Mapping Spectrometer (VIMS) Fomalhaut observation in C32. Since the pointing was already there, only datavolume and ISS instrument trigger and instrument load would have to be done. Unfortunately it was too late in the scheduling process to ride-along with VIMS. Long exposures would have to compare Spica with Fomalhaut.

Another concern was concerning the status of the WAC as no images were taken since C27, so a WAC image was added to the set with an exposure time from the ICO-1 observation for comparison.

### **C. C31 and C32 Activities**

A 3 weeklong activity was planned for C32, with some options for the second part of C32. In the February 12<sup>th</sup>, 2002 meeting it was decided to add a long heating cycle between the C30 and the planned C32 cycles with real-time commands. This 57-day long decontamination cycle began on DOY 064 (March 5) and ended on DOY 122 (May 2). There were no images taken as part of this sequence. It was inserted between the scheduled C30 and C32 decontaminations and was called "C30/C31 Phase 2." The "before" images from C32 were used to determine the effect of this decontamination. WAC images and 3 long-exposure NAC images were added to the C32 activity. To

further confirm that the contamination was not being completely removed at 4°C only to be re-condensed at lower temperatures, imaging at 4°C was added.

This 26-day long decontamination cycle with imaging began on DOY 129 (May 9) and ended on DOY 156 (June 5). The Spica images from C32 revealed that the optical performance of the NAC continued to improve over all wavelengths measured. Measurements showed that for the BL1/CL2 filter combination, where approximately 68% of the light was outside a radius of 5 pixels initially, it was now between 5 and 6%. This was back in the range of pre-anomaly values. Three sets of images were taken before the C32 decontamination, at  $-90^{\circ}$ ,  $-40^{\circ}$  and  $4^{\circ}$ . After the C32 decontamination, images were taken at  $4^{\circ}$  and  $-40^{\circ}$ . However, data dropouts due to problems with Deep Space Network (DSN) lockup caused 4 of the  $-90^{\circ}$  images to be lost completely and nearly all of the others had missing lines in the center of the image where Spica was located. The only two images containing Spica were seen and even they had problems. Since the CCD temperature did not go to  $-90^{\circ}$ C at the end of the C32 decontamination before increasing again, all of the analysis had to be done with the poorer quality  $-40^{\circ}$ C images. The size of the stellar profiles also clearly improved, with the BL1/CL2 combination at 2.46 pixels. The width of a star in many of the filter combinations were now in the range of pre-anomaly values. Comparing the “before” and “after” C32 images one could see that the 57-day C31 decontamination resulted in continued improvement while the 26-day C32 activity was inconsequential.

As described earlier, long exposures were added to the C32 activity to observe the very low level extended properties of the point-spread function in three filter combinations. These saturated long exposures were combined with the unsaturated shorter exposures to form a composite. The incredible stability of Cassini on Reaction Control Wheels allowed creating these composites. These composite images provided a much better determination of the effect of the C32 decontamination.

In order to compare the current state of the camera to its pre-anomaly state, a composite image was created using pre-anomaly C22 Fomalhaut data, the best dataset of long exposed stellar images. The C22 Fomalhaut sequence was done in the CL1/CL2 filter combination. Figure 8 shows the composite long exposure images for the UV1/CL2, CL1/CL2 and IR4/CL2 filters contrast enhanced to show their low level structure. The pre-anomaly Fomalhaut image on the left is scaled such that the total stellar DN is the same as the C32 images.

With better statistics afforded by the composite images, the affect of the C32 activity was detectable but minimal (hundredths of a pixel in size) and the stellar properties were still poorer than pre-anomaly values. But the comparison was not exact as these images were at the poorer  $-40^{\circ}$ C. Also, it was determined that the optics had not thermally stabilized before imaging. In the next decontamination sequence, the replacement heaters were turned off more than a day in advance to allow the optics to thermally stabilize. The next sequence also had  $-90^{\circ}$ C images again. The combination of those factors would tell the true state of the situation.

WAC images were added to this decontamination activity because no WACs had been taken since C27 (except dark frames and saturated scattered light images). There was a concern that there could be a possibility of cross contamination, because while the NAC was heated to drive off contamination, the WAC stayed cold and contamination migrates to cold surfaces. To check for this, images were taken duplicating a Violet Spica image taken during ICO-1 in January 1999. The WAC continued to show that it was unaffected.

The C32 decontamination activity was the first time in flight that images were taken at a CCD temperature of  $\sim 0^{\circ}$ C. Dark current and hot pixels dominated these images and the background was very noisy, making them not very useful for analysis. However, Bob West, a member of the ISS Science Team, indicated that dark frames at this temperature would be good for determining the camera’s uneven bit weighting correction. Such an observation was scheduled for the next activity. No evidence was seen that  $4^{\circ}$ C images were less contaminated than  $-40^{\circ}$ C ones.

In summary, the decontamination sequence undertaken in C31, which took the CCD to  $\sim +4^{\circ}$ C for two months, 8 times longer than previously, almost fixed the problem. The C32 decontamination, which heated the camera for an

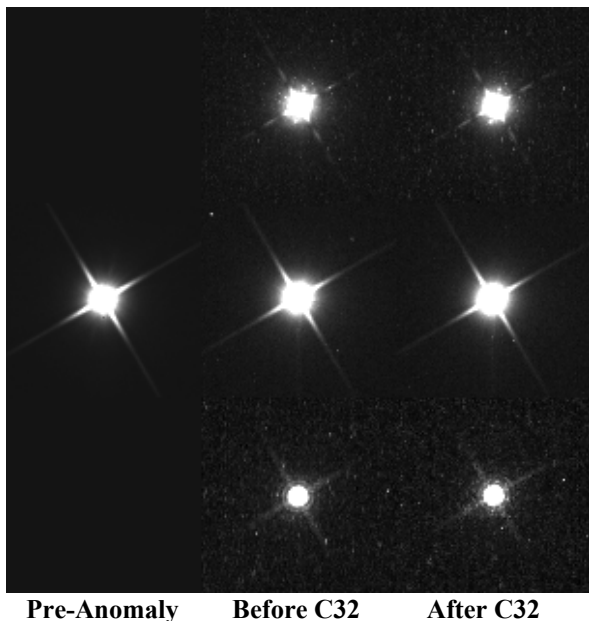


**Figure 8. Composite long exposure images at  $-40^{\circ}$ C.**

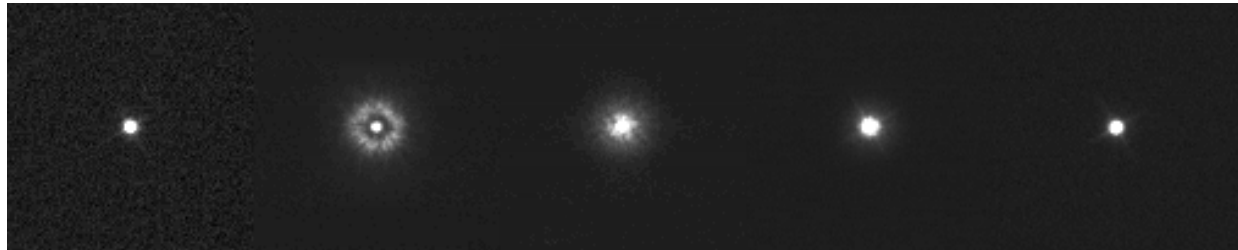
additional 26 days, caused little discernable additional improvement. We were now in the range where the analysis might be affected by the stability of the spacecraft pointing during observations.

#### D. C32/C33 Activity

This 34-day long decontamination cycle began on DOY 156 (June 5, 2002) and ended on DOY 190 (July 9). The Spica images from C33 revealed that the optical performance of the NAC improved only very slightly over nearly all wavelengths measured, when comparing images taken at  $-40^{\circ}\text{C}$  from the previous activity. The previous activity did not go to  $-90^{\circ}\text{C}$ .

The images in Fig. 9 show stellar images before the anomaly, after the anomaly, after the C28, C30 and C33 decontaminations, all in the same BL1/CL2 filters and adjusted for total stellar brightness. The images are all contrast enhanced in the same manner to show the faint extended light. All images were taken at  $-90^{\circ}\text{C}$ .

Measurements show that for this filter combination the amount of light outside a 5-pixel radius was 5%. If one



2001/145	2001/150	2001/299	2002/030	2002/190
Pre-Anomaly	Anomaly	C28	C30	C33
HD 339457	Maia in Pleiades	Spica	Spica	Spica
2.66	10.03	7.94	4.78	2.68
1.24	1.69	2.19	1.79	1.38
5.3%	68.7%	44.4%	17.9%	5.1%

**Figure 9. Comparison of stellar images in BL1/CL2 filter throughout the decontamination process. From the top is shown Year/Date, Event, Target, width using 25 pixel radius, width using 5 pixel radius, Percent of light outside 5 pixel radius.**

defines the “haze” as the extra light diffused out past a radius of 5 pixels as compared to pre-anomaly images, then the haze was gone. The sizes of the stellar profiles shown here are also nearly back to normal. The central peak was still somewhat wider than pre-anomaly for this filter. The central peak is from a few hundredths to around a tenth of a pixel larger in the other various filters tested. For the worst case, this is about 10% more than pre-anomaly (see Table 4).

Two sets of images were taken after the C32 decontamination, at  $-40^{\circ}$  and  $4^{\circ}\text{C}$ . After the C33 decontamination, images were taken at  $4^{\circ}$ ,  $-40^{\circ}\text{C}$  and  $-90^{\circ}\text{C}$ . Thus, the comparison to the results of the previous decontamination had to be done with  $-40^{\circ}\text{C}$  images. Composite images were again created. The Ultraviolet composite continued to show improvement over the last two activities, the Clear composite less so and the IR composite perhaps a tiny degradation but it is the most affected by noise.

#### E. Summary of results

Table 2 is a comparison of the Ratio of Halo flux to total Stellar flux for various filters. For images before the anomaly, the Ratio is from noise in the background and diffraction spikes. For images after the C28 decontamination, since there is no definitive halo, it is the fraction of light that falls in the area of the original halo. Measurements for all but the UV1/CL2 filter are the average of 3 images of HD 339457. The UV1/CL2 measurement was from a single Fomalhaut image in C22. For the RED/CL2 and IR4/CL1 filters, the images available with the halo were very faint and do not give good statistics, so both a Pleiades and Vega measurement is included. The effective wavelength listed for the filters was calculated using the ISS transmission curve integrated with a stellar spectrum similar to Spica (B2 III) in the Bruzual-Persson-Gunn-Stryker<sup>9</sup> atlas.

**Table 2. Ratio of ring component to total stellar flux. Asterisk indicates measurement at -40C.**

			Fomalhaut or HD 339457	Pleiades and/or Vega	Spica				
Filter	Eff wave, nm	Inner/ Outer radius, pix	Ratio before anomaly	Ratio after anomaly	Ratio after C28 decon	Ratio after C30 decon	Ratio* after C31 decon	Ratio* after C32 decon	Ratio after C33 decon
UV1/CL2	256	4 / 35	0.058	0.663	0.403	0.170	0.069	0.067	0.062
BL1/CL2	444	5 / 25	0.050	0.683	0.440	0.179	0.054	0.075	0.051
CL1/GRN	560	5 / 25	0.058	0.571	0.432	0.184	0.059	0.054	0.057
RED/CL2	641	5 / 28	0.066	<i>0.606</i> <i>0.455</i>	0.439	0.185	0.067	n/a	0.056
CL1/CL2	366	5 / 25	0.058	0.551	0.401	0.161	0.069	0.073	0.048
IR4/CL2	1000	5 / 30	0.119	<i>0.247</i> <i>0.333</i>	0.364	0.208	0.084	0.136	0.100

Table 3 is a comparison of the spread of the DN distribution. The first table shows the width calculated using pixels out to the outer halo radius. Images before the anomaly which have practically no signal near the outer radius, and -40°C images which are noisy can give very different values for size depending on what background value is used. Thus, this table does not include pre-anomaly images. For images that approach pre-anomaly values, the more stable values of size are those that only use pixels with a higher signal-to-noise ratio, such as the composite long-

**Table 3. Size of PSF using data out to outer halo radius. Asterisk indicates -40C measurement.**

			Pleiades and/or Vega	Spica Size calculated using pixels out to outer halo radius				
Filter	Eff wave (nm)	Outer radius (pix)	Size after anomaly	Size after C28 decon	Size after C30 decon	Size* after C31 decon	Size* after C32 decon	Size after C33 decon
UV1/CL2	256	35	14.53	7.37	5.32	2.15	1.73	2.87
BL1/CL2	444	25	10.03	7.94	4.78	2.46	3.76	2.68
CL1/GRN	560	25	9.59	6.89	4.75	2.84	2.50	2.98
RED/CL2	641	28	<i>13.06</i> <i>7.99</i>	7.70	4.89	3.36	n/a	3.08
CL1/CL2	366	25	10.04	8.25	4.77	3.16	3.59	2.65
IR4/CL2	1000	30	<i>8.48</i> <i>12.26</i>	7.64	6.26	4.08	5.98	4.63

exposure images. Thus, another table with size calculated using only pixels inside the inner halo radius is given, which shows both -40°C and -90°C for C33.

Table 4 uses pixels only out to the inner halo radius to calculate size. This is a measure of the width of the star ignoring the faint contributions far from the central peak.

**Table 4. Size of PSF using data out to inner halo radius. Asterisk indicates -40C measurement.**

			Fomalhaut or HD 339457	Spica Size calculated using pixels out to inner radius			
Filter	Eff wave, nm	Inner halo radius, pix	Size before anomaly	Size* after C31 decon	Size* after C32 decon	Size* C33 decon -40°C	Size C33 decon -90°C
UV1/CL2	256	4	1.15	1.24	1.25	1.22	1.18
BL1/CL2	444	5	1.24	1.40	1.46	1.44	1.38
CL1/GRN	560	5	1.28	1.41	1.43	1.43	1.38
RED/CL2	641	5	1.36	1.48	n/a	1.49	1.52
CL1/CL2	366	5	1.33	1.43	1.43	1.37	1.36
IR4/CL2	1000	5	1.63	1.62	1.63	1.62	1.66

#### F. End of Decontamination activities

Up to this point, the NAC had used 22 of the budgeted 57 thermal cycles for the mission. The risk of using a thermal cycle must be balanced with the diminished returns of perhaps a reduction in PSF width of a few hundredths of a pixel that another decontamination might accomplish. It was decided that risk of further decontaminations outweighed the small possible future gains. A planned C34 decontamination was cancelled. The images were still taken since it was too late to change the sequence, but a real time command to turn on the heaters was not sent. Analysis of these images showed no change, as expected.

A new flight rule written by J. Gerhard, not to allow both Level 1 and Level 2 heaters ON at the same time (prohibiting going to +30°C again) was implemented. With the start of Saturn Tour, no further decontaminations are planned unless a problem reoccurs. If a problem does reoccur, only a single set of heaters will be used, for long periods of time. This will obviously impact planned observations, unless a quiet time such as Superior Conjunction could be used. Continued monitoring shows no reoccurrence of the problem.

All these efforts by Instrument Operations, with the help of many others, helped ensure the success of the Cassini Saturn Tour. The next Saturn observation, in April 2003, was a success and was released to the public.

An unfortunate epilogue was reported in January of 2003. UVIS reported that the sensitivity of some of their EUV and FUV detector pixels were degraded by an amount up to 40%. They traced this back to May-June 2002 and the long stares at Spica associated with NAC haze anomaly resolution. Though this degradation could still be corrected via flat-fielding, procedures were implemented to avoid further problems from Spica and other bright stars.

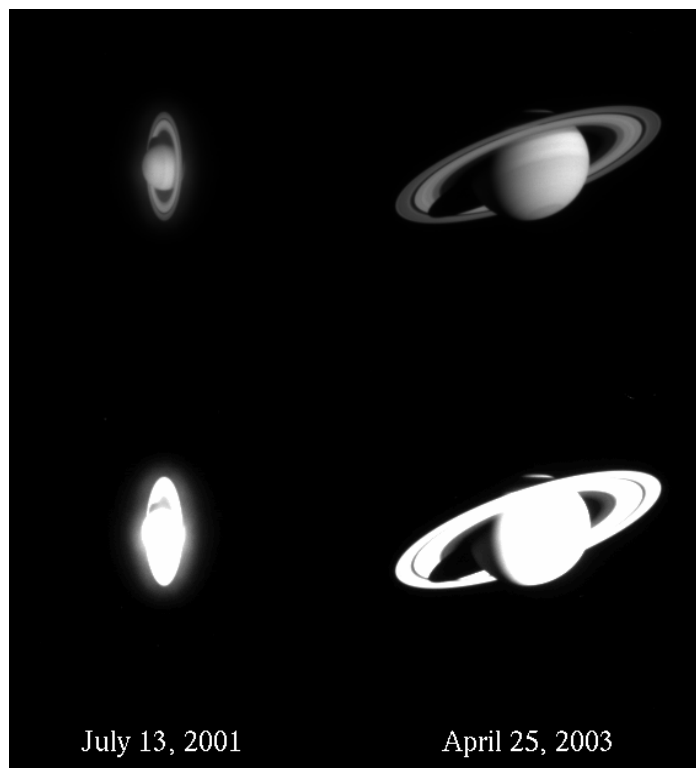


**Figure 10: The first two Saturn observations.**

## **VI. Lessons Learned**

### **A. Would have appreciated more flexibility in instrument design**

The decontamination heaters we had available were fixed and we could only combine them in certain ways to obtain quantized temperature values ( $-90^{\circ}$ ,  $-40^{\circ}$ ,  $0^{\circ}$  and  $+30^{\circ}\text{C}$ ). Using heaters in a non-planned way allowed us to go to  $+4^{\circ}\text{C}$ . We wanted to get to a temperature that the contamination engineers recommended (and cleared up Stardust) but we could not reach that temperature with what we had without going to the temperature that probably caused the problem. If the decontamination heaters were variable it would have given us more options.

### **B. Perform instrument calibration as early as possible**

Because the Jupiter encounter was a best-effort event and there was a limit on data volume, the science team decided to postpone in-flight photometric calibration until the pre-Saturn arrival cruise phase. This meant that the camera was not fully calibrated when the contamination event occurred and limited the pre-contamination comparisons we would have liked. It also prevented a poor-man's spectral analysis. Having an in-flight calibrated instrument is useful.

### **C. Have more flexibility in instrument operations**

Long lead times, limited datavolume and barriers to pointing the spacecraft complicated our efforts. Having to go through the Science team to plan activities was added work and an opportunity for errors to creep into the processes. The saving grace was the large amount of time before Saturn Tour to correct the problem. The ability to trade with other instruments helped us. The ability to image at non-operational CCD temperatures also helped us.

### **D. Anticipate possible anomalies and have pre-planned sequences to deal with them**

Because of the immature state of Cassini Operations and our uplink software during the cruise phase, it would have helped to have sequences already developed to generate the data needed to analyze the problem.

### **E. Have backup plans for data distribution during science team events**

The setup for data distribution to science team members involved data flow from JPL to the science team lead at CICLOPS and then from there to individual team members. It was unfortunate that the move of CICLOPS from Tucson to Boulder occurred about the time the anomaly happened. Science team members involved with instrument calibration did not notice the anomaly. The Cassini project now has the process set up to distribute data directly to the ISS science team members and many are taking advantage of the capability.

### **F. Keep an eye out on data quality**

Measure the size of stellar images and the sharpness of object edges if there are no stellar images often to detect changes in instrument response and catch problems early. Don't wait until right before a science opportunity to first try out an instrument, time may be needed for decontamination. For distributed operations define the responsibility for this monitoring and the reporting of problems. Especially pay attention to an event that has not been done before in flight.

### **G. Avoid large temperature ranges in decontamination**

The haze problem occurred after a decontamination activity with a temperature range of  $120^{\circ}\text{C}$ . Although there was no problem with the other camera over this same temperature range, thermal shock is known to generate contamination species so it may be wiser to spread such a temperature change over a long period of time.

## **Acknowledgments**

The research described in this paper was carried out at the Jet Propulsion Laboratory, California Institute of Technology, under a contract with the National Aeronautics and Space Administration. We would like to thank all

the members of the Cassini project that helped us get the NAC back on track: Glenn Aveni, Charlie Avis, Doug Dawson, Jerry Jones, Cindy Kahn, Lonnie Lane, Ellis Miner, Bill Owen, Tina Pavlicek, Dan Taylor, Brad Wallis, Robert West and others. We'd also like to express our appreciation to the Cassini SVT leads for their cooperation and the Stardust mission for insight on their problem.

### References

<sup>1</sup>Uy, O. M., et al., "Contamination Experiments in the Midcourse Space Experiment," *Journal of Spacecraft and Rockets*, Vol. 34, No. 2, March-April, 1997, pp. 218-225.

<sup>2</sup>Wilkes, D. R., Zwiener, J. M., "Optical Properties Monitor (OPM) in-situ experiment flown on the Mir station," *Proceedings of SPIE, Rough Surface Scattering and Contamination*, Vol. 3784, 1999, pp. 72-83.

<sup>3</sup>Bhaskaran, S., Mastrodemos, N., Riedel, J. E., Synnot, S. P., "Optical Navigation for the Stardust Wild 2 Encounter," *Proceedings of the 18<sup>th</sup> International Symposium on Space Flight Dynamics*, SP-548, ESA, 2004, pp. 455.

<sup>4</sup>Green, B. D., "Satellite Contamination and Materials Outgassing Knowledgebase – An Interactive Database Reference," *NASA Technical Report*, NASA/CR-2001-210909, March, 2001.

<sup>5</sup>Porco, C. C., et al., "Cassini Imaging Science: Instrument Characteristics and Anticipated Scientific Investigations at Saturn," *Space Science Reviews*, Vol. 115, 2004, pp. 363-497.

<sup>6</sup>Porco, C. C., et al., "Cassini Imaging of Jupiter's Atmosphere, Satellites and Rings," *Science*, Vol. 299, no. 5612, March 2003, pp. 1541-1547.

<sup>7</sup>Lock, P., Sarrel, M., "Distributed Operations for the Cassini/Huygens Mission," *Proceedings of SpaceOps98 Conference*, Tokyo, Japan, June 1998.

<sup>8</sup>Meyer-Arendt, J. R., Miner, E. D., "Optical Size Determinations on Models Resembling Malignant Tissue," *Laboratory Investigation*, Vol. 10, No. 4, July-August, 1961, pp. 826-836.

<sup>9</sup>See [http://www.stsci.edu/ftp/instrument\\_news/Observatory/cdbs/astronomical\\_catalogs.html](http://www.stsci.edu/ftp/instrument_news/Observatory/cdbs/astronomical_catalogs.html) .